

# Enhancement and Analysis of Heat Transfer Rate in Turbulent Flow through Tubes with Longitudinal Perforated X-Shaped Inserts

Md. Mizanuzzaman , Nusrat Jahan , Md. Almostasim Mahmud ,Salma Noor Jahan

**Abstract**— A high-performance heat exchanger of a fixed size can give an increased heat transfer rate. The objective of the paper is to study the heat transfer characteristics for forced convection through tube with longitudinal perforated X-shaped inserts. The experimental investigation has been carried out for turbulent flow in a circular tube with perforated x-shaped inserts with perforations of 0.0%, 5.7%, 10.15% and 15.87%. Air velocities, temperatures, tube wall temperatures were collected to analyze the Nusselt numbers, heat transfer coefficients, heat transfer rate, and heat transfer effectiveness for the plain tube as well as for the tube with inserts (both perforated and imperforated). The results indicated that as much as an average 2-4 fold and 1.4-2.9 fold improvement might be obtained in the turbulent flow heat transfer coefficient and the heat transfer effectiveness respectively for the tube with the perforated X-shaped inserts than for the plain tube and tube with X-shaped insert without perforation. With the experimental data, a correlation was also developed for prediction of the heat transfer coefficient and Nusselt number in turbulent flow for tubes with X-shaped inserts.

**Index Terms**— X-shaped insert porosity, Reynolds number, Nusselt number, heat transfer coefficients, heat transfer effectiveness, correlation.

## 1. INTRODUCTION

THE concept of forced convection heat transfer has many industrial applications. Every industry consists of heat exchanger, evaporator and condenser through which heat is transferred from one stream to another by forced convection. As a result, there has been strong demand for enhancement techniques of forced convection heat transfer. A high-performance heat exchanger of a fixed size can give an increased heat transfer rate. It might also cause a decrease in temperature differences between the process fluids enabling efficient utilization of thermodynamic availability. Many researchers have been studying the subject since the beginning of the twentieth century. Prince [1] obtained a 200% increase in the heat transfer coefficient with internal circumferential ribs; however, the outside (spray-film evaporation) was also enhanced. Hu and Chang [2] analyzed fully developed laminar flow in internally finned tubes by assuming constant and

empirically and evaluated by Gupte and Date [3] for twister tape-generated helical flow in annuli. Uddin [4] studied pressure drop characteristics and heat transfer performance of air through and internal rectangular finned tube. Mamun [5] experimentally investigated the heat transfer characteristics of steady-state turbulent fluid flow through an internally in-line segmented tube and a non-segmented finned tube at constant pumping power. Mozumder [6] studied experimentally the heat transfer performance of a T-section internal fin in a circular tube. Mohammad [7] numerically investigated the heat transfer augmentation for flow in a pipe or a channel partially or fully filled with perforated material placed at the core of the channel. Sarkar et al. [8] studied the heat transfer in turbulent flow through a tube with longitudinal strip inserts. Sarkar and Chowdhuri [9] were carried out an investigation to study the pressure drop, turbulent flow heat transfer in a tube with rod pin inserts. Ling and Chu [10] had done, 3D numerical simulations with internally roughened dimples in the range of  $Re = 2000$  to  $11,000$ . Hossein and Sayehvand [11] performed a detailed numerical study of laminar fully developed forced convection in a pipe partially filled with a porous medium. Sarkar and Mohammad [12] studied the turbulent flow convection heat transfer in a circular tube with perforated star-shaped mild steel inserts with perforations of 0.0%, 1.52%, 6.1%, 13.71%, and 24.37%. They found that as much as a two-fold improvement might be obtained in the turbulent flow heat transfer coefficient and the heat transfer effectiveness for the tube with the perforated star-shaped inserts than for the plain tube. Wazed, Ahmed and Sarkar [13] studied turbulent flow in a circular tube

- Md. Mizanuzzaman is currently working as an Instructor, Department of Mechanical Engineering, Military Institute of Science and Technology (MIST), Mirpur Cantomment, Dhaka1216, Bangladesh. Email: [mizan\\_zaman@yahoo.com](mailto:mizan_zaman@yahoo.com)
- Nusrat Jahan and Salma Noor Jahan , Researcher, Department of Mechanical Engineering, Military Institute of Science and Technology (MIST), Mirpur Cantomment, Dhaka1216, Bangladesh. Email: [nusratbubli@yahoo.com](mailto:nusratbubli@yahoo.com)
- Md. Almostasim Mahmud ,Ex. lecturer , Department of Mechanical Engineering, Military Institute of Science and Technology (MIST), Mirpur Cantomment, Dhaka1216, Bangladesh. Email: [mostasim\\_mist@yahoo.com](mailto:mostasim_mist@yahoo.com)

uniform heat flux in the tube surface. Friction and Nusselt number data were generated and semi-

with a porous/perforated twisted tape insert. Ventsislav and Bergles [14] were investigate the effect of corrugated tubes with twisted-tape inserts on the friction factors and heat transfer coefficients (inside with water as working fluid and outside with condensing steam) for single-phase turbulent flow.

However, a very limited number of data has been published on the thermo-hydraulic performance of tubes with x-shaped inserts of varying porosity.

Therefore our present study has been undertaken for a) To fabricate an experimental facility for studying turbulent flow heat transfer in a tube with perforated x-shaped inserts. b) To analyze the heat transfer performance. c) To develop a correlation that may be recommended for prediction of the heat transfer coefficient in tubes with perforated x-shaped inserts.

## 2 EXPERIMENTAL SETUP AND PROCEDURE

The experimental facility consists of Test section, Inlet section, Air supply system and Heating arrangement.

### 2.1 Tube and Insert Configuration

The whole experimental facility consists of a circular tube which has mainly three sections inlet section, test section and outlet section. The unheated inlet section is about 2 m long and 3 mm thick mild steel circular tube having outer diameter of 60mm. The test section is 1.5 m long mild steel circular tube having the same diameter of inlet section and is placed between inlet and outlet section. Inserts are placed inside the test section. The test section was divided into two equal parts along its length. Inserts are the main important parts of the experimental facility.

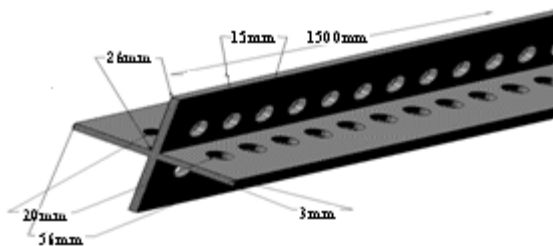


Fig. 1. 3D view of X-shaped perforated insert[15]

There were total four inserts we used in our experiment which having X-shape and in case of four inserts, each plate is at  $90^\circ$  with each other. All the inserts are 1.5 m long. One insert was kept plain i.e. it had no porosity or  $R_p=0\%$ . Other inserts are having porosity of 5.7%, 10.15%, 15.87%. Porosity is the ratio of total pore or hole area on the surface to the total surface area of the insert. For all the inserts mild steel sheet of 3 mm thickness had been used during the experiment. Figure-4.3 shows a

perforated X-shaped insert with dimension. Hole diameter is varied from 4 mm to 8 mm with the pitch of 15 mm longitudinally and 20 mm at transverse direction. Outlet section is about 2 m long having the same dimension of inlet section. One end of outlet section is connected with test section and another end is connected with the blower section. The blower section provides the supply of air to the circular tube which is connected at the end of the outlet section. An electrically operated and induced draft centrifugal blower was placed downstream from the test section to draw air which was used for this purpose.

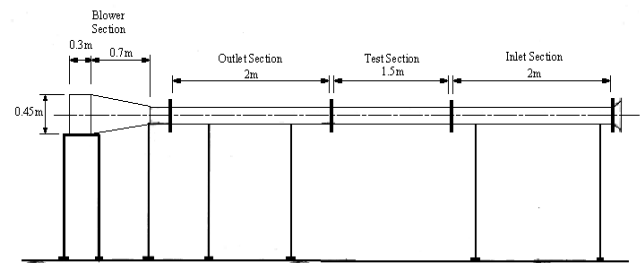


Fig. 2. Experimental Facility with Inlet section, Test section, Outlet Section and Blower section [15].

### 2.2 Setup Procedure

A pitot static tube was placed on the inlet section at a distance of about 1.5 m from air inlet. An inclined tube manometer was connected to the pitot static tube to measure the velocity of. The outlet section was at first bolted with the diffuser of the blower section. A butterfly valve was placed inside the outlet section and just before the blower. The diameter of the insert was kept slightly larger than the inside diameter of the smooth tube after machining process so that the insert could be tightly fitted against the wall tube. At first insert with percentage of porosity 0% was placed into one half of the test section. After placing the insert axially into one half of the semi-cylindrical plain tube, the two halves of the plain tube were bolted together. In order to prevent leakage rubbers were placed into the joint of the tube before bolting. The test section was then bolted with the inlet and the outlet section through collar or flanges. Asbestos gaskets and also rubber sheets were used in between two flanges to prevent heat flow to the longitudinal direction and also to prevent leakage of air. Similarly, three test sections were arranged for the other three inserts with different porosity of 5.7%, 10.15% and 15.87%[15].

After preparing and connecting the test section with experimental facility, it was covered with mica sheet to provide electrical insulation. Then nichrome wire (with a resistance of 18 ohm/m) which acts as an electrical heater was spirally wound uniformly with a spacing of 16 mm around the tube. Then thermocouples were placed at different position on the test section.



Fig. 3. Tube with perforated insert[15].

One thermocouple was placed at the inlet section and another was placed transversely at the outlet section through a drilling hole. Again the mica sheet, glass fiber, heat insulating tape and asbestos tape were sequentially put over the nichrome wire heater coil to prevent radial heat losses.

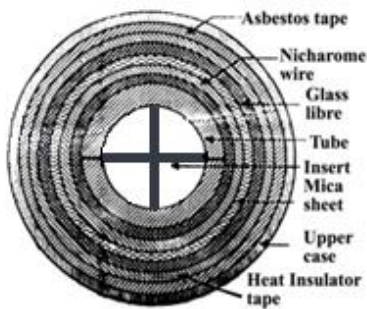


Fig. 4. Transverse Cross Sectional View of the Test Section [15].

When covering the test section with fiber glass, heat insulation tape, and asbestos tape was completed then all the thermocouples are connected with selector switch which is connected with a temperature display by a common point..

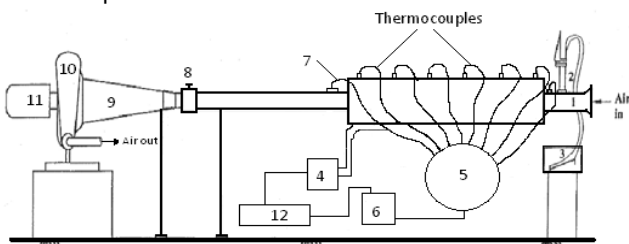


Fig. 5. Schematic diagram of the experimental facility in which; 1. Inlet section, 2. Traversing pitot static tube, 3. Inclined tube manometer, 4. Variable voltage transformer, 5. Selector switch, 6. Temperature display, 7. Traversing thermocouple, 8. Butterfly valve, 9. Diffuser, 10. Blower, 11. Motor, 12. AC Power Supply[15].

The two ends of nichrome wire were connected with the variable transformer. AC power was supplied to the variable transformer and the temperature display. Figure-5 shows the schematic diagram of experimental setup



Fig. 6. Experimental Setup[15]

## 2.3 Experimental and Measuring Procedure

The data collected during the experiment on the basis of following assumptions-

a) Inside diameter of the tube ( $D_i$ ) is used instead of hydraulic diameter ( $D_h$ ) in defining Reynolds number and Nusselt number. b) All the fluid properties are calculated at fluid mean bulk temperature instead of film temperature and at atmospheric pressure instead of local pressure in the test section, which is slightly less than the atmospheric pressure. c)  $T_o$  is assumed to vary linearly along the length of the test section, where  $T_s$  varies nonlinearly along the length of the tube. d) The heat is transferred only by forced convection from inside wall of the tube to the fluid. However, there may have some conduction heat transfer through the tape from wall due to the contact of the tape with the wall. Heat is also conducted through the ends of the test section to the adjacent section.

Following steps were followed during the measuring procedure.

At first the fan was switched on and allowed to run continuously for 10 minutes to obtain steady-state conditions. Initially the butterfly valve was kept at 0° position. By the pitot static tube along with the inclined tube manometer air velocity was measured at this position. The air flow rate could be varied through the test section by varying the angle of opening of the butterfly valve.

Then the electric heater was switched on and during whole experiment a constant power was maintained (1000 Watts) with the help of variable transformer or variac.

After that we observed the temperatures at different point on the test section. At the beginning wall temperatures varied until constant values were attained. Whether the steady state condition was attained or not, this could be sure by observing the outlet temperature. The steady state condition was attained when the outlet air temperature did not fluctuate over a 10-15 minutes time period.

At the steady state condition the wall temperature remained stationary at different locations of the test

section. As the steady state condition was attained thermocouple readings were recorded manually with the help of a selector switch.

After taking the reading for butterfly position at 0o, the same procedure was repeated until the butterfly position was reached at 90o through opening the butterfly valve by 10o at each case. For each 10o opening manometric reading was taken.

### 3 ANALYSIS OF HEAT TRANSFER

For analysing the heat transfer rate local surface temperature at different position on the test section were taken and local bulk temperatures were calculated. The data obtained were used to find the local and average heat transfer coefficient and local and average Nusselt number.

#### 3.1 Analysis of Local Heat Transfer Coefficient

Local heat transfer coefficient can be calculated by using the following formula-

$$h_x = \frac{q_s}{(T_{sx} - T_{bx})}$$

Figure-7 shows, local heat transfer coefficient along the length of the test section for both smooth tube and tube with X-shaped inserts which can be compared with tube with X-shaped longitudinal strip insert [8]. The curves for smooth tube and tube with X-shaped insert without perforation are almost similar to tube with X-shaped longitudinal strip insert [8]. For smooth tube and tube with X-shaped insert local heat transfer coefficient is high at the entrance region and at the exit region. From the entrance region it decreases gradually up to the dimensionless distance of  $x/L = .411$ . Then it increases up to the exit region of the test section. Because at the entrance the presence of a gasket and leading edge creates a vortex inside the test section while at the outlet conduction heat transfer occurs through the non-insulated connecting tube. But in case of tubes with perforated insert local heat transfer coefficient increases gradually along the length. This is occurred due to very less vortex created at the entrance; hence local heat transfer coefficient is not higher at the entrance significantly in compared with the middle region of the test section and increased gradually along the length. Result also shows that, local heat transfer coefficient for tube with X-shaped insert without perforation is 1.20-3.9 times lower than the smooth tube. For tube with insert of porosity,  $R_p = 5.7\%$  local heat transfer coefficient is 1.18-2.8 times higher than the smooth tube and 1.12-5.5 fold compared to insert without perforation. For insert of porosity,  $R_p = 10.15\%$  Local heat transfer coefficient is 1.10-7.72 fold compared to smooth tube and 1.45-9 fold compared to insert without perforation.

By using the calculated data following graphs are obtained-

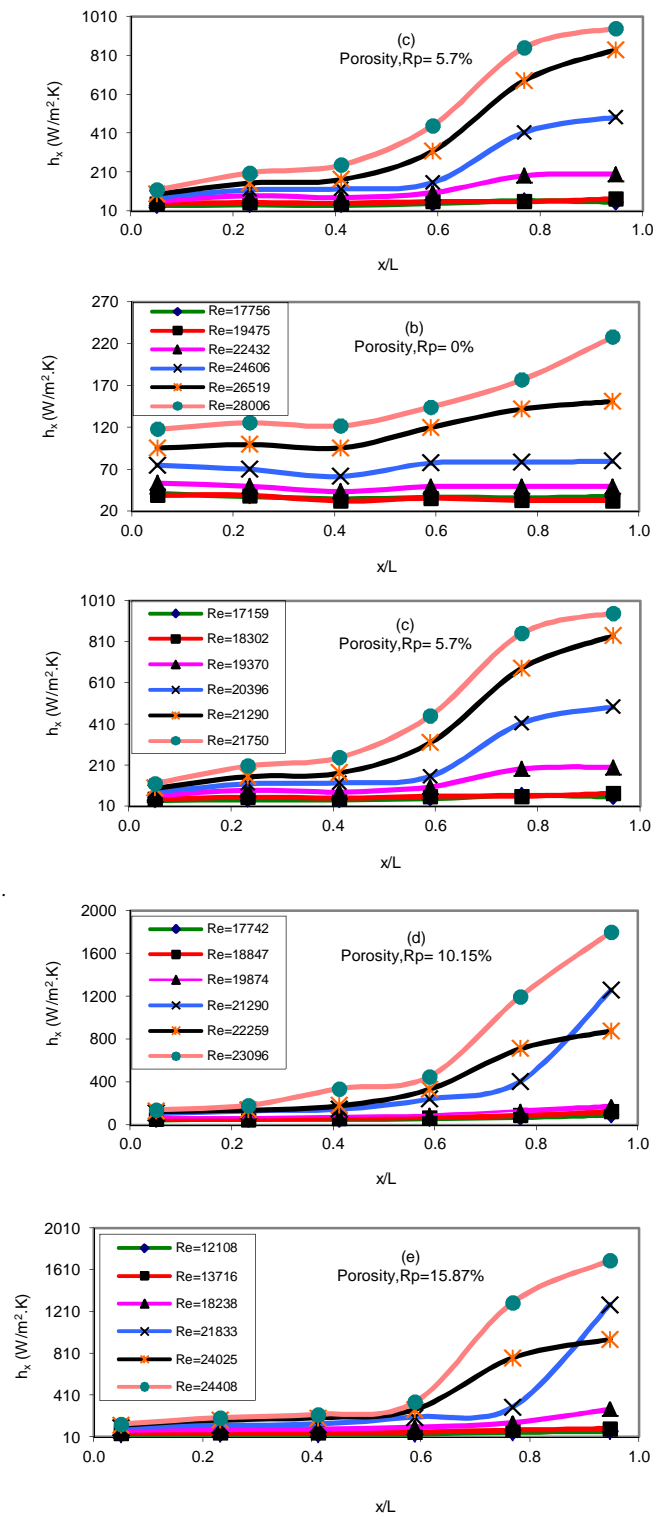


Fig. 7. Local heat transfer coefficient ( $h_x$ ) along the length of the test section for tubes with inserts of different porosity (a-e).

For tube with insert of porosity,  $R_p = 15.87\%$  local heat transfer coefficient is highest and it is 1.15-8 fold compared to smooth tube and 1.15-9.8 fold compared to insert without perforation. From figure, it is also shown that in



the five cases local heat transfer coefficient increases with Re.

### 3.2 Analysis of Average Heat Transfer Coefficient

By using the local heat transfer coefficient, average heat transfer coefficient at different Re are obtained and following graph is plotted.

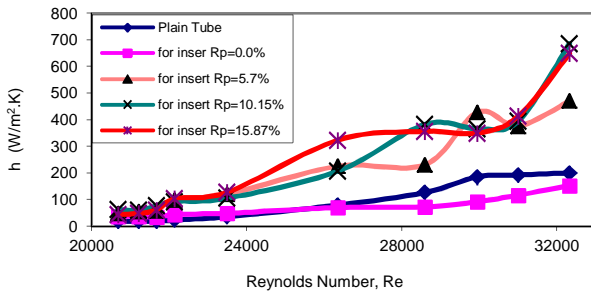


Fig. 8. Comparison of average heat transfer coefficient with Reynolds number for both smooth and X-shaped longitudinal strip inserted tube.

Figure-8 shows, the average heat transfer coefficient change with Re for both smooth tube and tube with X-shaped inserts. Result shows that, average heat transfer coefficient for tube with insert of porosity,  $R_p=0\%$  is 1.5 times lower than the smooth tube. For tube with insert of porosity,  $R_p=5.7\%$  average heat transfer coefficient is about 2.5 fold compared to smooth tube and about 3 fold compared to insert without perforation. For insert of  $R_p=10.15\%$  average heat transfer coefficient is about 2.8 fold compared to smooth tube and about 2-4 fold compared to insert without perforation. For  $R_p=15.87\%$  average heat transfer coefficient is highest and is 3 fold compared to smooth tube and 2-4.8 fold compared to insert without perforation. Figure also shows that, average heat transfer coefficient is increased with the increasing of Re.

### 3.3 Analysis of Local Nusselt Number

Figure 9 show local Nu along the length of the test section for both smooth tube and tube with X-shaped inserts which can be compared with tube with X-shaped longitudinal strip insert [8]. The curves for smooth tube and tube with X-shaped insert without perforation are almost similar to tube with X-shaped longitudinal strip insert [8]. For smooth tube and tube with X-shaped insert local Nu is high at the entrance region and at the exit region. From the entrance region it decreases gradually up to the dimensionless distance of  $x/L=0.411$ . Then it increases up to the exit region of the test section. This is occurring for the same reason as discussed for local heat transfer coefficient, since local Nu is a function of local heat transfer coefficient.

By using the calculated local heat transfer coefficients local Nusselt numbers are obtained and following graphs are plotted-

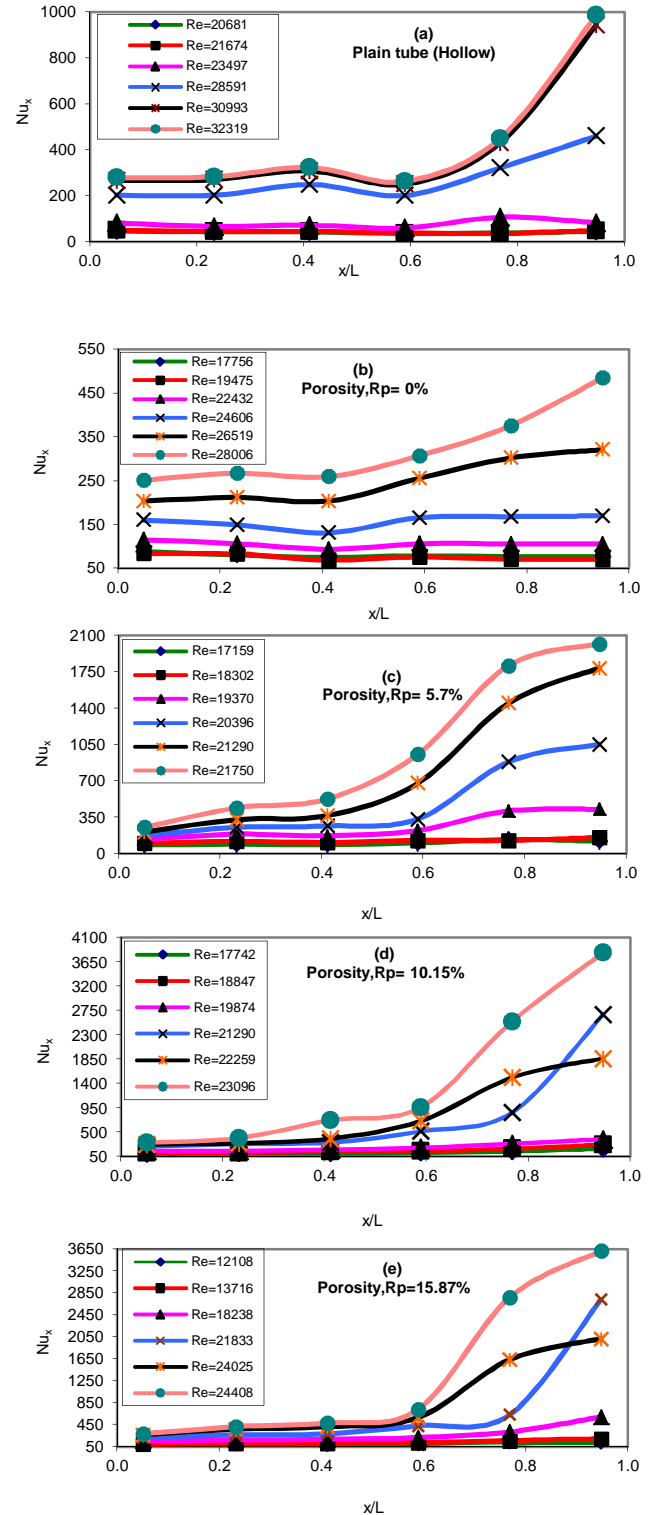


Fig. 9. Local Nusselt number along the length of the test section for tubes with X-shaped inserts of different porosity

Result also shows that, local Nu for tube with X-shaped insert without perforation is 1.20-3.8 times lower than

the smooth tube. For tube with insert of porosity,  $R_p=5.7\%$  local Nu is 1.18-2.9 fold compared smooth tube and 1.12-5.5 fold compared to insert without perforation. For insert of porosity,  $R_p=10.15\%$  local Nu is 1.10-7.7 fold compared to smooth tube and 1.5-9 fold compared to insert without perforation. For tube with insert of porosity,  $R_p=15.87\%$  local Nu is highest and it is 1.15-8 fold compared to smooth tube and 1.15-9 fold compared to insert without perforation. From figure, it is also shown that in the five cases local Nu increases with Re.

### 3.4 Analysis of Average Nusselt Number

The average Nusselt numbers are obtained from local Nusselt number for different Re and following graph is plotted.

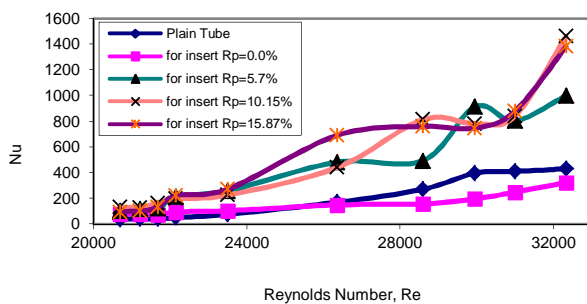


Fig. 10. Comparison of average Nusselt number with Reynolds number for both smooth tube and tubes with X-shaped inserts.

Figure-10 shows the average Nu change with Re for both smooth tube and tube with X-shaped inserts. Result shows that, average Nu for tube with insert of porosity,  $R_p=0\%$  is 1.5 times lower than the smooth tube. For tube with insert of porosity,  $R_p=5.7\%$  average Nu is about 2.5 fold compared to smooth tube and about 3 fold compared to insert without perforation. For insert of  $R_p=10.15\%$  average Nu is about 2.8 fold compared to smooth tube and about 2-4 fold compared to insert without perforation. For  $R_p=15.87\%$  average Nu is highest and is 3 fold compared to smooth tube and 2-4.8 fold compared to insert without perforation. Figure also shows that average Nu is increased with the increasing of Re.

From the above graphs, local and average Nusselt number, and local and average heat transfer coefficient are quite similar to the tube with X-shaped longitudinal strip insert [8]. From observing the graphs, it is clear that heat transfer is higher for tube with perforated inserts than the smooth tube and the tube with insert of 0% perforation. Figures also show that heat transfer is decreased for tube with insert 0% perforation than the smooth tube. This is occurred due to the decreased diameter of the test section than the inlet section created by machining work which causes less heat transfer to air due to decreased air flow through the test section. But for tube with perforated insert rate of heat transfer increased due to swirling effect of air and increased turbulence while passing through tubes due to the

porosity of insert although the diameter of test section is decreased than the inlet and outlet section and causes less air flow rate.

## 4 DEVELOPING A HEAT TRANSFER CORRELATION

From figures 9-10, it is clear that Nusselt number for smooth tube and tube with X-shaped inserts (with perforation and without perforation) is a function of the Re and percentage of porosity. Hence these may be correlated by following Colburn equation-

$$Nu = C Re^m \cdot Pr^{0.33}$$

Or

$$\frac{Nu}{Pr^{0.33}} = C Re^m$$

Or

$$\ln\left(\frac{Nu}{Pr^{0.33}}\right) = \ln(C Re^m)$$

Or

$$\ln\left(\frac{Nu}{Pr^{0.33}}\right) = \ln C + m \ln Re \quad (1)$$

Equation (1) can be compared with the equation of straight line,

$$y = mx + c$$

Where,

$$y = \ln\left(\frac{Nu}{Pr^{0.33}}\right), \quad x = \ln Re$$

$m$ =slope of the straight line,  $c = \ln C = \text{constant}$

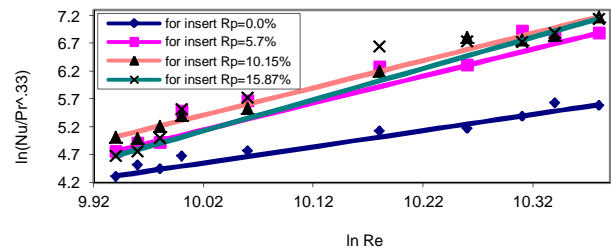


Fig. 11. Least square lines representing the correlation of Nusselt number for X-shaped inserts with different porosity.

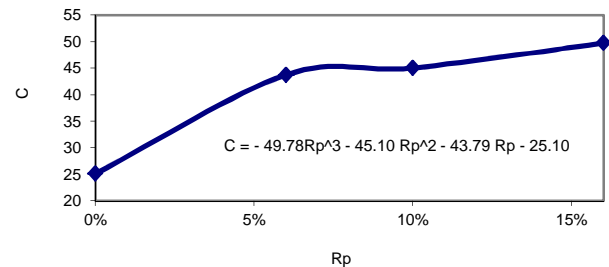


Fig. 12. Variation of C with the percentage of porosity (Rp) for X-shaped inserts.

Figure-11 shows, the straight lines representing the correlations for smooth tube and tube with insert for both with perforation and without perforation. The

slopes of straight line  $m$  and the value of constant  $C$  are obtained from figure. The values for constant  $C$  and  $m$  are plotted against  $R_p$  in figures 12 and 13.

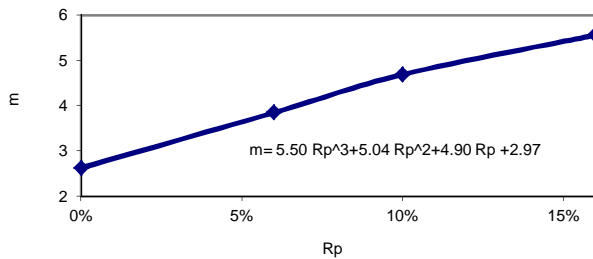


Fig. 13. Variation of  $m$  with the percentage of porosity ( $R_p$ ) for X-shaped inserts.

Hence the variation of constant  $C$  and  $m$  with  $R_p$  are represented by the polynomial equations as given below,

$$C = -49.78R_p^3 - 45.10R_p^2 - 43.79R_p - 25.10 \quad (2)$$

$$m = 5.50R_p^3 + 5.04R_p^2 + 4.90R_p + 2.97 \quad (3)$$

Therefore, the final correlation of  $Nu$  for the tubes with X-shaped inserts is as follows,

$$Nu = (-49.78R_p^3 - 45.10R_p^2 - 43.79R_p - 25.10) \times Re^{5.50R_p^3 + 5.04R_p^2 + 4.90R_p + 2.97} \times Pr^{0.33} \quad (4)$$

## 5 ANALYSIS OF HEAT TRANSFER EFFECTIVENESS

By considering the wall temperature as constant and the same throughout the entire heated section, the effectiveness in both the smooth tube and the tubes with x-shaped inserts can be calculated using the following equation-

$$\varepsilon = \frac{T_{bo} - T_{bi}}{T_s - T_{bi}}$$

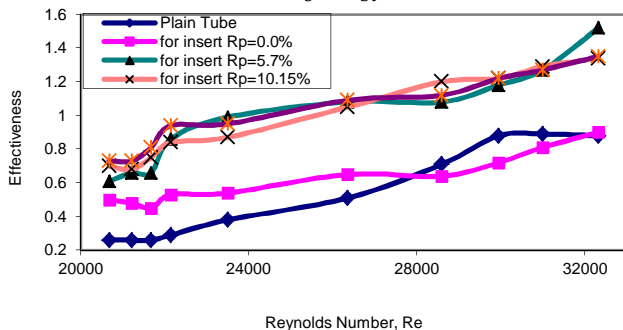


Fig. 14. Comparison of effectiveness with Reynolds number for both smooth tube and tube with X-shaped inserts

Figure-14 shows, that effectiveness is higher for tubes with x-shaped inserts than for smooth tube. For tube with insert of 0% perforation is 1.9 times higher the

smooth tube, for tube with insert of porosity,  $R_p=5.7\%$  effectiveness is 1.4-2.6 fold and 1.2-1.7 fold compared to smooth tube and tube with 0% perforation, for tube with insert of porosity,  $R_p=10.15\%$  effectiveness is 1.3-2.9 fold and 1.4-1.9 fold compared to smooth tube and tube with 0% perforation and for tube with insert of porosity,  $R_p=15.85\%$  effectiveness is 1.4-3.2 fold and 1.5-1.8 fold compared to smooth tube and tube with 0% perforation. Therefore we have seen that higher effectiveness is obtained for porosity,  $R_p=15.85\%$ .

## 6 CONCLUSION

Turbulent tube flow is widely used in various industrial applications and the available correlation of heat transfer are mostly of empirical or semi empirical nature. In recent years energy and material saving consideration have prompted and expansion of the efforts aimed at producing more efficient heat exchanges equipment through the augmentation of heat transfer. In our study an experimental investigation has been carried out to study the augmentation of heat transfer for turbulent flow in a circular tube with X-shaped inserts (both perforated and non-perforated). The study has shown that, the perforated X-shaped inserts caused an increase of heat transfer and effectiveness. The present study can be considered as the basis of further work associated with the enhancement of heat transfer and apply it to design optimum and effective heat exchanger. For further study following steps can be recommended-

- Pressure drop and the friction factor can be at different point in the test section for further analysis, because the increase in heat transfer with augmentation is accompanied by an increase in the friction factor.
- Further analysis can be done for higher perforation of the inserts and observe the heat transfer characteristics.
- Study of required pumping power for airflow through the test section can be determined.
- There are always some uncertainties in every experimental process. Therefore; further study of this experiment may contain the uncertainty analysis of different parameters.
- Further analysis of the heat transfer characteristics for tube with x-shaped inserts can be done with high speed fluid or liquid such as water.
- Metal used for insert was mild steel, which is more corrosive and having more weight, therefore the study can be done with some other materials which are less corrosive and reduce the weight of test section.

## NOMENCLATURE

Re Reynolds number ( $\rho vD/\mu$ )  
Pr Prandtl number ( $\mu C_p/k$ )  
Nu Average Nusselt number ( $hD_i/k$ )  
Nux Local Nusselt Number  
hx Local heat transfer coefficient (W/m<sup>2</sup>.K)  
h Average surface heat transfer coefficient (W/m<sup>2</sup>.K)  
k Thermal conductivity of fluid or air (W/m.K)  
Rp Percentage of porosity of the X-shaped insert (ratio of total pore area in the insert to the total surface area of the insert)  
D=Di Inside diameter of the test section (m)  
v Mean velocity of fluid (m/s)  
x Any position along the length of the test section (m)  
qs Surface heat flux (W/m<sup>2</sup>)  
Tbx Local Bulk temperature of the fluid (°C)  
Tsx Local Surface temperature of the pipe or tube (°C)

#### Subscripts

Tbi Inlet bulk temperature of air (°C)  
Tbo Outlet bulk temperature of air (°C)  
Ts Average Surface temperature of the pipe or tube (°C)  
p Porous/perforated tube  
x Local

#### Greek Symbols

$\rho$  Density of air (kg/m<sup>3</sup>)  
 $\mu$  Absolute Viscosity (N.s/ m<sup>2</sup>)  
 $\epsilon$  Effectiveness of the heat exchanger

#### REFERENCES

- [1] Prince, W.J. ,Enhanced tubes for horizontal evaporation desalination process, *MS thesis*, Department of Engineering, University of California at Los Angeles,1971.
- [2] Hu, M.H. and Chang, Y.P., Optimization of finned tubes for heat transfer in laminar flow, *J. Heat Transfer*, vol. 95, pp.332-338, 1973.
- [3] Gupte, N. S. and Date, A. W., Friction and heat transfer characteristics of helical turbulent air flow in annuli, *J. Heat Transfer*, vol. 111, pp.337-344, 1989.
- [4] Uddin, J.M., Study of Pressure drop characteristics and heat transfer performance in an internally finned tube, *MS thesis*, Department of Mechanical Engineering, Bangladesh University of Engineering and Technology, 1999.
- [5] Mamun, A.H.M., Pressure drop and heat transfer in an internally finned tube, *MS thesis*, Department of Mechanical Engineering, Bangladesh University of Engineering and Technology, 1999.
- [6] Mozumder, A. K., Heat transfer performance of internally finned tube, *MS thesis*, Department of Mechanical Engineering, Bangladesh University of Engineering and Technology, 2001.
- [7] Mohamad, A.A., Heat transfer enhancement in heat exchanger fitted with perforated media.Part 1: Constant wall temperature, *Int. J. Heat Mass Transfer*, vol. 42, pp. 385-395, 2003.
- [8] Sarkar, M.A. R., Hasan, A.B.M.T., Ehsan, M., Talukdar, M. M. A. and Huq, A.M.A., Heat transfer in turbulent flow through tube with longitudinal strip inserts, *Proc. of International Conference on Mechanical Engineering*, Dhaka, Bangladesh, ICME05-TH-46, pp. 1-6, 2005a.
- [9] Sarkar, M.A.R., Chowdhuri, M.A. K, Hossain, R.A., Islam, S.M. N, Heat transfer in turbulent flow through tube with rod-pin inserts, *Proc. of International Conference on Mechanical Engineering*, Dhaka, Bangladesh, ICME07-TH-02, 2007.
- [10] Li, R., He, Ya-Ling, Lei, Y. G., Tao , Y. B., Chu, P. A Numerical Study on Fluid Flow and Heat Transfer Performance of Internally Roughened Tubes with Dimples , DOI: 10.1615, *J. Enh. Heat Transfer*.vol. 16. i3. 40, pp. 267-285, 2009.
- [11] Shokouhmand, H., Sayehvand, H., Study of Forced Convection in a Pipe Partially Filled with a Porous Medium DOI: 10.1615, *J. Enh. HeatTransfer*.vol. 17. i3.10, pp. 205-221, 2010.
- [12] Sarkar, M. A. R., Sarkar, A.M. and Mohammad, A. M., Heat Transfer and Pressure Drop in Turbulent Flow through a Tube with Longitudinal Perforated Star-Shaped Inserts, DOI: 10.1615, *J. Enh. Heat Transf.*2011001859, pp. 491-502, 2011.
- [13] Wazed, M.A., Ahamed, J. U., Ahmed, S., Sarkar, M. A. R., Enhancement of Heat Trabsfer in Turbulent Flow through a Tube with a Perforated Twisted Tape Insert, DOI: 10.1615, *J. Enh. Heat Transf.* vol. 18. i1.10, pp. 1-13, 2011.
- [14] Zimparov, V., Petkov V. M., Bergles A. E., Performance Characteristics of Deep Corrugated Tubes with Twisted-Tape Inserts, *J. Enhanced Heat Transfer*, vol. 19, i. 1, pp. 1-11, 2012.
- [15] Md. Mizanuzzaman , Nusrat Jahan, Amina Ahmed , Md.Mahmud, Experimental Study of Temperature Distribution in Turbulent Flow through Tubes with Longitudinal Perforated X-Shaped Inserts, *IJETAE*, Vol 3, Issue 1, 2013, pp 24-30.